Adaptive Conjugate Smoothing of Discontinuous Fields

Minvydas Ragulskis and Violeta Kravcenkiene

Kaunas University of Technology,
Department of Mathematical Research in Systems,
Studentu st. 50, Kaunas, Lithuania

Abstract. A technique for adaptive conjugate smoothing of discontinuous fields is presented in the paper. The described technique is applicable in various engineering problems and is especially effective when hybrid numerical - experimental methodologies are used. Adaptive smoothing strategy is illustrated for a discontinuous plain stress field problem when photoelastic fringes representing the variation of stress are constructed in virtual projection plane.

Keywords: Finite element method, adaptive smoothing, visualization

1 Introduction

Adaptive smoothing of discontinuous fields is a problem of a high importance in hybrid numerical - experimental techniques when the results of experimental analysis are mimicked in virtual numerical environment [1]. Typical example is the construction of digital fringe images from finite element analysis results imitating the stress induced effect of photo-elasticity [2].

Conventional finite element analysis is based on interpolation of nodal variables (displacements) inside the domain of each element [3]. Though the field of displacements is continuous in the global domain, the field of stresses is discontinuous at inter-element boundaries due to the operation of differentiation. Construction of digital fringe images from finite element analysis results is a typical problem when discontinuous fields are to be visualized. Therefore it is important to develop numerical techniques enabling physically based smoothing applicable for visualization procedures.

The proposed strategy of smoothing parameter is based on the assumption that the larger smoothing is required in the zones where the discontinuity of the field is higher.

The finite element norm representing the residual of stress field reconstruction in the domain of the analyzed element is introduced. It can be noted that the calculation of element norms is not a straightforward procedure. First, the nodal stress values in the global domain are sought by the least square method minimizing the differences between the interpolated stress field from the nodal stress values and discontinuous stress field calculated directly from the displacement field. As the minimization is performed over the global domain and the

Z. Li et al. (Eds.): NAA 2004, LNCS 3401, pp. 463–470, 2005.

interpolations are performed over the local domains of every element, direct stiffness procedure based on Galiorkin method is developed and applied to the described problem.

When the nodal stress values are calculated, the finite element norms are calculated for each element as the average error of the field reconstruction through the interpolation of those nodal values.

It can be noted that the first step of calculation of the nodal values of stress produces a continuous stress field of stresses over the global domain. Nevertheless that field is hardly applicable for visualization procedures as the derivatives of the field are discontinuous and the plotted fringes are unsmooth. Therefore the augmented residual term is added to the previously described least squares procedure while the magnitudes of the terms for every finite element are proportional to the element norms. Explicit analysis of the smoothing procedure for the reconstruction of the stress field is presented for a one-dimensional problem.

Digital images of two-dimensional systems simulating the realistic effect of photoelasticity are presented. Those examples prove the importance of the introduced smoothing procedure for practical applications and build the ground for the development of hybrid numerical experimental techniques.

2 FEM Based Technique for Adaptive Conjugate Smoothing

Stress component σ (a continuous function) inside a finite element can be calculated in a usual way [3]:

$$\sigma = [D]\{\varepsilon\} \tag{1}$$

where $\{\varepsilon\}$ – column of generalized nodal strains of the analysed finite element; $[D]$ – vector row relating the strain component and nodal strains in the domain of the finite element. Vector $[D]$ involves the derivatives of the element's shape functions in conventional FEM models based on displacement formulation [3]. Therefore, though the displacement field is continuous in the global domain, the strain field can be discontinuous at the inter-element boundaries [3].

Techniques used for the visualization of results from FEM analysis [4] require the nodal values of the plotted parameter which are interpolated in the domain of each finite element by its shape functions. Therefore visualization of the stress field requires data on the nodal values of the stress. This is not a straightforward problem for conventional FEM formulations.

Probably the natural way for calculation of nodal values of stress would be the minimization of residual constructed as an integral of the squared difference between the interpolated and factual stress fields over the global domain:

$$\sum_{D.S.} \left(\iint \left([N]\{s\} - \sigma \right)^2 dxdy \right) \tag{2}$$

where abbreviation $D.S.$ stands for FEM direct stiffness procedure [5]; integrals are calculated over the domain of each finite element; $[N]$–row of the shape func-

tions of finite element;$\{s\}$ – column of unknown nodal values of the component of stress in currently integrated finite element.

Though such reconstruction of stress field solves the problem of discontinuity, the derivatives of the stress field are still discontinuous at inter-element boundaries. Visualization procedures for such types of interpolated fields are highly sensitive to such discontinuities of derivatives [4]. Therefore there exists a need to design a method for smoothing the reconstructed field.

The proposed method is based on the augmentation of the residual (3) by a penalty term for fast change of the stress in any direction in the analysed plane:

$$\lambda_i \left(\left(\frac{\partial \sigma}{\partial x} \right)^2 + \left(\frac{\partial \sigma}{\partial y} \right)^2 \right) \tag{3}$$

where $\lambda_i > 0$ are smoothing parameters selected individually for every finite element. Keeping in mind that the stress field is interpolated by the form functions of the finite element the augmentation term can be approximately interpreted as

$$\left(\frac{\partial w}{\partial x} \right)^2 + \left(\frac{\partial w}{\partial y} \right)^2 \approx \{s\}^T [C]^T [C] \{s\} \tag{4}$$

where

$$[C] = \begin{bmatrix} \frac{\partial N_1}{\partial x} & \frac{\partial N_2}{\partial x} & \cdots & \frac{\partial N_n}{\partial x} \\ \frac{\partial N_1}{\partial y} & \frac{\partial N_2}{\partial y} & \cdots & \frac{\partial N_n}{\partial y} \end{bmatrix}$$

and n–number of nodes in the analyzed element; N_i – shape functions of the $i-th$ node.

Then the nodal values of stress are found minimizing the augmented residual:

$$\frac{d\left(\sum_{D.S.} \left(\iint \left(([N]\{s\} - \sigma)^2 + \lambda_i \{s\}^T [C]^T [C] \{s\} \right) dxdy \right) \right)}{ds_i} = 0, \tag{5}$$

where $i = 1, \ldots, m$, s_i is an $i-th$ component ($i-th$ nodal value) of global vector of nodal values of strain $\{S\}$; m - number of nodes in the global domain. Step-by-step differentiation leads to following equality:

$$\sum_{D.S.} \left(\iint \left([N]^T [N] + [C]^T \lambda_i [C] \right) dxdy \right) \cdot \{S\} = \sum_{D.S.} \left(\iint [N]^T \sigma dxdy \right) \tag{6}$$

It can be noted that eq. 6 is a system of linear algebraic equations in respect of unknown nodal values of $\{S\}$. Moreover, this formulation conveniently involves the smoothing parameter λ into FEM formulation. $\sum_{D.S.}(\iint [N]^T [N] dxdy)$ is a positive definite matrix in conventional FEM [5], so the system matrix in eq. 6 will be also positive definite at $\lambda > 0$, what will guarantee the solution of $\{S\}$. Finally, eq. 6 is very convenient for implementation, straightforwardly falls into FEM ideology and therefore does not require extensive modifications of standard FEM codes.

3 One-Dimensional Example

The properties of conjugate smoothing can be illustrated by the following trivial example. One-dimensional system consisting from three elements and four nodes

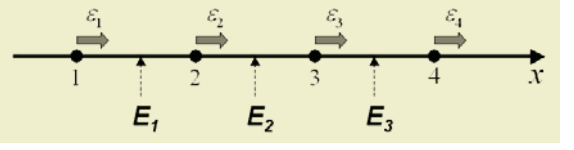

Fig. 1. One-dimensional system consisting from 3 linear finite elements and 4 nodes

is presented in Fig. 1. For simplicity it is assumed that the elements are linear, co-ordinates of the nodes x_k are:

$$x_k = k - 1, \qquad k = 1, \ldots, 4 \tag{7}$$

Then the shape functions of the $i-th$ element are:

$$\begin{aligned} N_1^{(i)}(x) &= i - x \\ N_2^{(i)}(x) &= x - i + 1, \end{aligned} \tag{8}$$

Here $i = 1, \ldots, 3$.

The nodal strains are explicitly defined as ε_k. Strain distribution in the domain of the $i-th$ finite element is approximated by appropriate shape functions:

$$\varepsilon^{(i)}(x) = N_1^{(i)}(x)\varepsilon_i + N_2^{(i)}(x)\varepsilon_{i+1} \tag{9}$$

Then the stress inside the $i-th$ element is calculated as the derivative of strain [2]:

$$\sigma^{(i)}(x) = B_1^{(i)}(x)\varepsilon_{(i)} + B_2^{(i)}\varepsilon_{i+1} = \varepsilon_{i+1} - \varepsilon_{(i)} \tag{10}$$

where

$$B_1^{(i)}(x) = \frac{\partial N_1^{(i)}(x)}{\partial x} = -1 \qquad B_2^{(i)}(x) = \frac{\partial N_2^{(i)}(x)}{\partial x} = 1 \tag{11}$$

The unknown nodal values of stress are denoted as s_k. It can be noted that $[N] = \left\lfloor N_1^{(i)}(x); N_2^{(i)}(x) \right\rfloor$; $[C] = \left\lfloor B_1^{(i)}(x); B_2^{(i)}(x) \right\rfloor$. Then, for the $i-th$ element:

$$\begin{aligned} \int_{i-1}^{i} [N]^T[N]dx &= \int_{i-1}^{i} \begin{bmatrix} \left(N_1^{(i)}(x)\right)^2 & N_1^{(i)}(x)N_2^{(i)}(x) \\ N_1^{(i)}(x)N_2^{(i)}(x) & \left(N_2^{(i)}(x)\right)^2 \end{bmatrix} dx = \begin{bmatrix} \frac{1}{3} & \frac{1}{6} \\ \frac{1}{6} & \frac{1}{3} \end{bmatrix} \\ \int_{i-1}^{i} [C]^T[C]dx &= \int_{i-1}^{i} \begin{bmatrix} \left(B_1^{(i)}\right)^2 & B_1^{(i)}B_2^{(i)} \\ B_1^{(i)}B_2^{(i)} & \left(B_2^{(i)}\right)^2 \end{bmatrix} dx = \begin{bmatrix} 1 & -1 \\ -1 & 1 \end{bmatrix} \\ \int_{i-1}^{i} [N]^T\sigma^{(i)}(x)dx &= \int_{i-1}^{i} \begin{bmatrix} N_1^{(i)}(x)\sigma^{(i)}(x) \\ N_2^{(i)}(x)\sigma^{(i)}(x) \end{bmatrix} dx = \begin{bmatrix} \frac{\varepsilon_{i+1}-\varepsilon_i}{2} \\ \frac{\varepsilon_{i+1}-\varepsilon_i}{2} \end{bmatrix} \end{aligned} \tag{12}$$

Initially it is assumed that the smoothing parameter λ is the same for all elements. Direct stiffness procedure [5] over the three elements results into the following system of linear algebraic equations:

$$\begin{bmatrix} \frac{1}{3}+\lambda & \frac{1}{6}-\lambda & 0 & 0 \\ \frac{1}{6}-\lambda & \frac{2}{3}+2\lambda & \frac{1}{6}-\lambda & 0 \\ 0 & \frac{1}{6}-\lambda & \frac{2}{3}+2\lambda & \frac{1}{6}-\lambda \\ 0 & 0 & \frac{1}{6}-\lambda & \frac{1}{3}+\lambda \end{bmatrix} \cdot \begin{bmatrix} s_1 \\ s_2 \\ s_3 \\ s_4 \end{bmatrix} = \begin{bmatrix} \frac{\varepsilon_2-\varepsilon_1}{2} \\ \frac{\varepsilon_3-\varepsilon_1}{2} \\ \frac{\varepsilon_4-\varepsilon_2}{2} \\ \frac{\varepsilon_4-\varepsilon_3}{2} \end{bmatrix} \tag{13}$$

The solution of this linear system can be found using computer algebra:

$$\begin{aligned} s_1 &= \frac{36\lambda^2(\varepsilon_4-\varepsilon_1)-12\lambda(8\varepsilon_1-6\varepsilon_2-3\varepsilon_3+\varepsilon_4)-19\varepsilon_1+24\varepsilon_2-6\varepsilon_3+\varepsilon_4}{3(36\lambda^2+36\lambda+5)} \\ s_2 &= \frac{36\lambda^2(\varepsilon_4-\varepsilon_1)-6\lambda(10\varepsilon_1-3\varepsilon_2-6\varepsilon_3-\varepsilon_4)-7\varepsilon_1-3\varepsilon_2+12\varepsilon_3-2\varepsilon_4}{3(36\lambda^2+36\lambda+5)} \\ s_3 &= \frac{36\lambda^2(\varepsilon_4-\varepsilon_1)-6\lambda(\varepsilon_1+6\varepsilon_2+3\varepsilon_3-10\varepsilon_4)+2\varepsilon_1-12\varepsilon_2+3\varepsilon_3+7\varepsilon_4}{3(36\lambda^2+36\lambda+5)} \\ s_4 &= \frac{36\lambda^2(\varepsilon_4-\varepsilon_1)+12\lambda(\varepsilon_1-3\varepsilon_2-6\varepsilon_3+8\varepsilon_4)-\varepsilon_1+6\varepsilon_2-24\varepsilon_3+19\varepsilon_4}{3(36\lambda^2+36\lambda+5)} \end{aligned} \tag{14}$$

The reconstructed stress in the domain of the $i-th$ element is approximated by the shape functions of the $i-th$ element:

$$S^{(i)}(x,\lambda) = s_i(\lambda)N_1^{(i)}(x) + s_{i+1}(\lambda)N_2^{(i)}(x) \qquad i = 1,\ldots,3 \tag{15}$$

It can be noted that

$$\lim_{\lambda\to\infty}\big(s_1(\lambda)\big) = \lim_{\lambda\to\infty}\big(s_2(\lambda)\big) = \lim_{\lambda\to\infty}\big(s_3(\lambda)\big) = \lim_{\lambda\to\infty}\big(s_4(\lambda)\big) = \frac{\varepsilon_4-\varepsilon_1}{3} \tag{16}$$

By the way, application of computer algebra simplifies the calculation of the following integral:

$$\sum_{i=1}^{3}\left(\int_{i-1}^{i} S^{(i)}(x,\lambda)dx\right) = \varepsilon_4-\varepsilon_1 \tag{17}$$

Remarkable is the simplicity of the result and the fact that the integral does not depend from λ . By the way,

$$\sum_{i=1}^{3}\left(\int_{i-1}^{i}\sigma^{(i)}(x)dx\right) = \sum_{i=1}^{3}\left(\int_{i-1}^{i}(\varepsilon_{i+1}-\varepsilon_i)dx\right) = \varepsilon_4-\varepsilon_1 \tag{18}$$

The produced equalities (14) and (15) enable construction of smoothed field of stresses in the analyzed domain. Further improvement of the smoothing technique is possible when the smoothing parameters are selected individually for each element. Such adaptive selection is based on the magnitude of error norms of the elements which are calculated as:

$$R_i = \sqrt{\int_{i-1}^{i}\left(N_1^{(i)}(x)s_i(0) + N_2^{(i)}(x)s_{i+1}(0) - \sigma^{(i)}(x)\right)^2 dx} \tag{19}$$

It can be noted that in determination (20) the nodal values of stress $s_i(0)$ and $s_{i+1}(0)$ require the solution of eg. (13) at $\lambda = 0$. Calculation of the error norms enables the selection of individual parameters of smoothing:

$$\lambda_i = aR_i \tag{20}$$

where a is a constant. Direct stiffness procedure will produce the following system of algebraic equations:

$$\begin{bmatrix} \frac{1}{3}+aR_1 & \frac{1}{6}-aR_1 & 0 & 0 \\ \frac{1}{6}-aR_1 & \frac{2}{3}+a(R_1+R_2) & \frac{1}{6}-aR_2 & 0 \\ 0 & \frac{1}{6}-aR_2 & \frac{2}{3}+a(R_2+R_3) & \frac{1}{6}-aR_3 \\ 0 & 0 & \frac{1}{6}-aR_3 & \frac{1}{3}+aR_3 \end{bmatrix} \cdot \begin{bmatrix} s_1 \\ s_2 \\ s_3 \\ s_4 \end{bmatrix} = \begin{bmatrix} \frac{\varepsilon_2-\varepsilon_1}{2} \\ \frac{\varepsilon_3-\varepsilon_1}{2} \\ \frac{\varepsilon_4-\varepsilon_2}{2} \\ \frac{\varepsilon_4-\varepsilon_3}{2} \end{bmatrix} \tag{21}$$

It is clear that the solution of eq.21 at $a = 0$ will coincide with the solution of eq.13 at $\lambda = 0$. Computer algebra helps to prove that

$$\lim_{a\to\infty}\big(s_1(a)\big) = \lim_{a\to\infty}\big(s_2(a)\big) = \lim_{a\to\infty}\big(s_3(a)\big) = \lim_{a\to\infty}\big(s_4(a)\big) = \frac{\varepsilon_4-\varepsilon_1}{4} \tag{22}$$

at bounded error norms R_i.

Assumption of particular values of strains - for example $\varepsilon_1 = 0.02$; $\varepsilon_2 = 0.02$; $\varepsilon_3 = 0.06$ and $\varepsilon_4 = -0.02$ enables the illustration of the reconstructed field of stress. The nodal values of strain at $\lambda = 0$ are: $s_1 = -0.083$; $s_2 = 0.045$; $s_3 = 0.021$; $s_4 = -0.131$. The error norms of the elements are: $R_1 \approx 0.0426667$; $R_2 \approx 0.0471781$; $R_3 \approx 0.0506667$.

Then the system of equations 22 can be solved at different values of a and the calculated nodal values of stress can be interpolated by the shape functions in the domain of every element. The results are visualized in Fig. 2. It can be noted that the reconstructed field of stress at $a = 0$ is continuous in the global domain, but the discontinuity of its derivatives at inter-element boundaries is an obstacle for construction of its smooth visual interpretations. Increase of parameter a helps solving this problem what is illustrated in the following section.

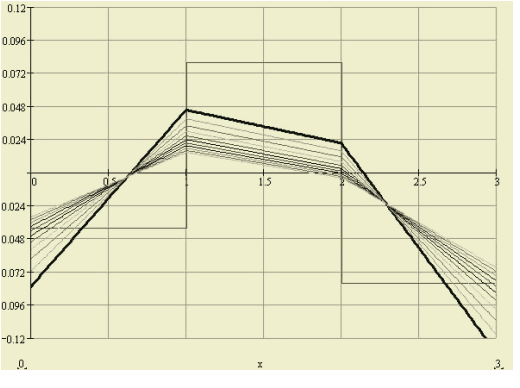

Fig. 2. Reconstructed field of stress S at $a = (i-1)*0.25$; $i = 1, \ldots, 20$; the horizontal lines represent σ

4 Adaptive Smoothing for Stress Field Visualisation in the Problem of Plane Stress

The components of stresses in the domain of the analysed finite element are calculated in the usual way [2, 5]:

$$\left\{ \begin{array}{c} \sigma_x \\ \sigma_y \\ \tau_{xy} \end{array} \right\} = [D][B]\{\delta_0\} \tag{23}$$

where $\{\delta_0\}$ is the vector of nodal displacements of the analysed element; $[B]$ is the matrix relating the strains with the displacements; $[D]$ is the matrix relating the stresses with the strains; σ_x, σ_y, τ_{xy} are the components of the stresses in the problem of plane stress. Conjugate smoothing of the stress field in the global domain results in the following system of equations:

$$\begin{aligned} \Big(\sum_i \iint\limits_{e_i} \big([N]^T[N] + [C]^T \lambda_i [C]\big) dxdy \Big) \cdot \{\delta_x\} &= \sum_i \iint\limits_{e_i} [N]^T \sigma_x dxdy \\ \Big(\sum_i \iint\limits_{e_i} \big([N]^T[N] + [C]^T \lambda_i [C]\big) dxdy \Big) \cdot \{\delta_y\} &= \sum_i \iint\limits_{e_i} [N]^T \sigma_y dxdy \\ \Big(\sum_i \iint\limits_{e_i} \big([N]^T[N] + [C]^T \lambda_i [C]\big) dxdy \Big) \cdot \{\delta_{xy}\} &= \sum_i \iint\limits_{e_i} [N]^T \tau_{xy} dxdy \end{aligned} \tag{24}$$

where $\{\delta_x\}$ - the vector of nodal values of σ_x; $\{\delta_y\}$ - the vector of nodal values of σ_y; $\{\delta_{xy}\}$ - the vector of nodal values of τ_{xy}. Relative error norms for finite elements are calculated using the methodology described in Eq.(21) and averaging for all three components of plain stress.

5 Computational Example and Concluding Remarks

Practical applicability and usefulness of the presented technique for adaptive smoothing of discontinuous fields is illustrated by the following example where the discontinuous stress field is visualised generating digital image of isochromatics in virtual projection plane. The numerical procedure used for constructing digital fringes is presented in [4]. Three patterns of fringes corresponding to the same strain field are presented in Fig. 3. Unsmoothed fringes are presented in Fig. 3a. It can be clearly seen that the structure of fringes is not uniform at the inter-element boundaries what is especially distinct in the corners of the area. Fig. 3b presents uniformly smoothed fringes. Though the structure of the pattern is smoother than in Fig. 3a, the fringes in the corners are missing. That corresponds to an over-smoothed state and illustrates a non-physical behaviour of the system. Fig. 3c corresponds to adaptive smoothing where the value of parameter λ is selected in accordance to finite element norms as described earlier.

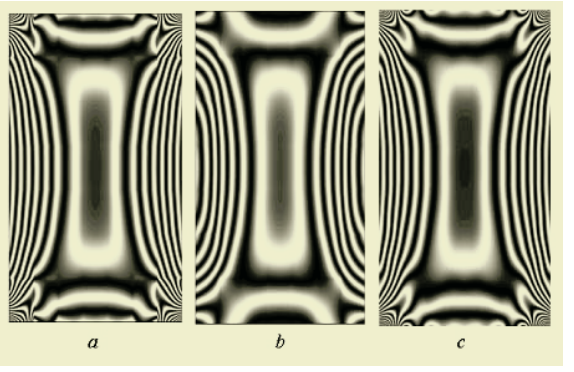

Fig. 3. Photoelastic fringes for a plane stress problem: a–unsmoothed fringes at $\lambda = 0$; b–smoothed fringes at constant $\lambda = 0,1$ for all elements; c–fringes after adaptive smoothing

The whole pattern of fringes is rather smooth, while the corner fringes are not eliminated.

Presented smoothing technique can be applied in different engineering applications. Especially it is useful in hybrid numerical - experimental techniques where the functionality of the systems is mimicked in virtual computational environment and the represented field of physical parameters is discontinuous.

References

1. Holstein A., Salbut L., Kujawinska M., Juptner W.: Hybrid Experimental-numerical Concept of Residual Stress Analysis in Laser Weldments. Experimental Mechanics, 41(4), 343-350 (2001).
2. Dally J.W., Riley W.F.: Experimental Stress Analysis. McGraw Hill Book Company, New York (1991).
3. Atluri S.N., Gallagher R.H., Zienkiewicz O.C., Eds.: Hybrid and Mixed Finite Element Methods. John Wiley & Sons (1983).
4. Ragulskis M., Palevicius A., Ragulskis L.: Plotting Holographic Interferograms for Visualisation of Dynamic Results From Finite Element Calculations. International Journal for Numerical Methods in Engineering, 56(11), 1647-1659 (2003).
5. Bathe K.J.: Finite element procedures in engineering analysis. New Jersey: Prentice-Hall, 1982. - p. 738.